NASA TECHNICAL NOTE

NASA TN D-4879

NASA TN D-4879

RADIOFREQUENCY TRANSMISSION CHARACTERISTICS OF SEVERAL ABLATION MATERIALS

by Melvin C. Gilreath, William F. Croswell, and Stark L. Castellow, Jr.

Langley Research Center
Langley Station, Hampton, Va.

NATIONAL AERONAUTICS AND SPACE ADMINISTRATION • WASHINGTON, D. C. • NOVEMBER 1968

NASA TN D-4879

RADIOFREQUENCY TRANSMISSION CHARACTERISTICS OF SEVERAL ABLATION MATERIALS

By Melvin C. Gilreath, William F. Croswell,
and Stark L. Castellow, Jr.

Langley Research Center
Langley Station, Hampton, Va.

NATIONAL AERONAUTICS AND SPACE ADMINISTRATION

For sale by the Clearinghouse for Federal Scientific and Technical Information
Springfield, Virginia 22151 – CFSTI price $3.00

RADIOFREQUENCY TRANSMISSION CHARACTERISTICS OF SEVERAL ABLATION MATERIALS

By Melvin C. Gilreath, William F. Croswell,
and Stark L. Castellow, Jr.
Langley Research Center

SUMMARY

An experimental investigation was conducted to determine the transmission loss, and effects upon the radiation patterns and impedance of typical antennas, produced by thermally degraded ablation materials. A cone-shaped model was used, which consisted of a truncated aluminum substructure with flush-mounted antennas over which a thermal-protection test material was bonded. Measurements of transmission loss through several thermal-protection materials were made at 2.66 GHz and 9.60 GHz in apparatus C of the Langley entry structures facility (an atmospheric arc jet).

The dielectric properties of all virgin materials were measured at room temperature. In addition, antenna radiation patterns, voltage standing wave ratios (VSWR), and gain were determined before and after the materials were subjected to the thermal test. Photographs of the models are presented which show the effects of the thermal test on the various materials.

It is concluded that, in general, materials which form and retain continuous conductive char layers during thermal exposure produce very high transmission losses. Also, it is shown that antennas which are covered with such high-loss materials may exhibit extreme perturbations in the radiation patterns that are not present when the antenna is covered with the virgin material.

The antennas used for this test program experienced an increase in VSWR when covered with the high-loss materials; however, the loss attributable to this mismatch was less than 2 dB.

INTRODUCTION

The antennas of reentry vehicles must be protected from the severe heating conditions encountered during entry into and exit from a planetary atmosphere. In order to maintain communications to receiving stations after the severe heating ceases, the

degraded thermal protection material covering the antennas must not seriously attenuate radiofrequency energy propagated through it nor severely alter the antenna radiation characteristics.

Dielectric ablation materials are developed primarily for heat-protection purposes. Hence, general information about the thermal protection characteristics of such materials is obtained during the developmental process. Some information on the electrical characteristics (i.e., transmission-loss measurements) of thermally degraded ablation materials is presently available (refs. 1 and 2). However, to select an ablation material for use as an antenna cover or window, a transmission-loss number in decibels (related to material thickness and operating frequency), without other supporting measurements, may not be sufficient. In this paper the following measurements are presented and evaluated:

(a) Measurement of the dielectric properties of the virgin materials at room temperature

(b) Measurement of the antenna characteristics (gain, radiation patterns, impedance) of the test model covered with virgin material

(c) Measurement of the transmission losses through the material after exposure to simulated entry heating conditions

(d) Measurement of antenna characteristics of the test model after exposure to the simulated entry conditions

The primary test frequencies were 2.66 GHz and 9.60 GHz. The frequency of 2.66 GHz was chosen because of available equipment near the space communication band of 2.2 to 2.4 GHz. The frequency of 9.60 GHz was chosen because of its inherent increased sensitivity to ablation effects and characteristics.

SYMBOLS

E	electric field
$f_{r,0}$	resonant frequency of unloaded cavity
$f_{r,l}$	resonant frequency of loaded cavity
H	magnetic field
Q_0	quality factor of unloaded cavity at resonance

Q_l	quality factor of loaded cavity at resonance
S	S-band frequency range, 2.60 GHz to 3.95 GHz
S_f	S-band forward power
S_r	S-band reflected power
t	thickness of test material
t_s	thickness of test material, measured in wavelengths in the dielectric medium, at 2.66 GHz
t_x	thickness of test material, measured in wavelengths in the dielectric medium, at 9.60 GHz
tan δ	loss tangent of dielectric medium
X	X-band frequency range, 8.20 GHz to 12.4 GHz
X_f	X-band forward power
X_r	X-band reflected power
ϵ_r	relative dielectric constant
λ_ϵ	wavelength in dielectric medium
θ	polar angle in spherical coordinate system
ϕ	azimuth angle in spherical coordinate system

TEST CONDITIONS AND PROCEDURES

Measurement of Dielectric Properties of Virgin Materials at Room Temperature

The dielectric properties of several ablation materials were measured by using the lowest order mode rectilinear-cavity method (ref. 3). A number of transverse

electric (TE_{101}) dominant mode cavities were constructed with unloaded resonant frequencies from 3.0 GHz to 14.0 GHz. Coaxial probes with the center conductor machined flush to the cavity walls were used for coupling the energy into and out of the cavity. This arrangement provided an undercoupled cavity with an unloaded insertion loss greater than 25 dB. The dielectric constant and loss tangent were obtained by measuring the resonant frequency and the associated quality factor for both the unloaded and loaded cavity conditions. From reference 3,

$$\epsilon_r = \left(\frac{f_{r,0}}{f_{r,l}}\right)^2$$

and

$$\tan \delta = \frac{1}{Q_l} - \frac{1}{Q_0}\left(\frac{f_{r,0}}{f_{r,l}}\right)^{1/2}$$

where $f_{r,0}$ and Q_0 are the unloaded cavity parameters, and $f_{r,l}$ and Q_l are the loaded parameters. The resonant frequencies were measured by an interpolation method (ref. 4, pp. 386-389). The response curves of the cavities were measured by the substitution method, also given in reference 4 (pp. 403-405).

Test Facility

Apparatus C of the Langley entry structures facility has the following capabilities:

(a) Produces model afterbody cold-wall heating rates of 20 to 50 Btu/ft^2-sec $(227$ to 567 kW/m$^2)$, typical of those encountered on the afterbody of a blunt entry vehicle

(b) Accommodates a test model of sufficient volume for mounting test antennas, cables, waveguide, and thermocouples

(c) Permits an experimental arrangement such that transmission-loss measurements can be accomplished

The details of the construction and operation of this facility are given in reference 5. This arc jet is characterized by subsonic flow and an enthalpy of approximately 3000 Btu/lb (6973 kJ/kg). Both the stream velocity and enthalpy available from this facility are lower than those that would be encountered by a typical blunt entry vehicle.

For these tests the nozzle diameter was 6 inches (15.24 cm) and the arc power was 1.8 megawatts with the following average stream conditions:

Airflow rate	0.35 lb/sec (0.16 kg/sec)
Stream enthalpy	2800 Btu/lb (6508 kJ/kg)
Velocity	2700 ft/sec (823 m/sec)
Temperature	3700° K
Mach number	0.07
Pressure	Atmospheric

These test conditions gave the desired cold-wall heating rate of approximately 20 to 50 Btu/ft^2-sec (227 to 567 kW/m^2) over the afterbody length.

Test Models

Upon selection of the test facility, the largest model that the facility could accommodate was chosen. Figures 1 and 2 show pertinent dimensions and construction details of the basic model used in all tests. The test materials were 0.25 inch (0.635 cm) in thickness and were bonded to the aluminum substructures. (See table I.) Care was taken to remove the bond material over the antenna apertures. The nose cap was either phenolic asbestos or, for one E4A1 model, a low-density phenolic nylon.

The X-band horn antenna (excited by a rectangular waveguide operating in the dominant TE_{10} mode) shown in figures 1(a) and 2 was used both as an antenna and as a means of connecting the model to the water-cooled sting. The sting has an internal X-band waveguide and a 0.750-inch (1.905-cm) hollow tube, both of which extend the entire length of the sting. The hollow tube is used for the passage of coaxial cables and thermocouple wires. The S-band antenna (figs. 1(b) and 2) is a T-bar cavity filled with glass-fiber laminate. The two test antennas (horn and T-bar cavity) are of the broadband type and are not detuned significantly when covered with the test materials.

There were eight thermocouple connections inside the test model, located at four different stations (labeled TC in fig. 1(a)). A graphite ring (figs. 1 and 2) was used to protect the rear of the model and to provide a fairing between the test model and the sting. Since the graphite ring was a good thermal conductor, it had to be insulated from the aluminum substructure by a bakelite ring (figs. 1 and 2). This insulator reduced the transfer of heat into the rear of the test model.

Instrumentation and Measurement Procedure

A block diagram of the instrumentation used for making the transmission-loss measurements is shown in figure 3. A signal generator which was calibrated in frequency and power output was modulated with a 1 kHz square wave and used to drive a traveling-wave-tube amplifier (TWTA) to give an output power of 1 watt. This signal was transmitted by coaxial cable or waveguide through the water-cooled sting to the

model. Dual directional couplers were used to monitor the forward and reflected power levels. The forward power was monitored during each test to indicate any change in generator output power. The reflected power was recorded continuously during each test. The signal was transmitted from the test-model antenna and received by a standard-gain horn antenna positioned to receive maximum signal level. A crystal detector at the receiving antenna detected the signal, which was then recorded. The recorder had a 40 dB dynamic range and a chart drive system that was adjusted to provide the desired speed for the test. Eight thermocouples in the model were connected through the water-cooled sting to a calibrated recorder to give the temperatures inside the model.

A series of measurements was made on each model just before the thermal test. These consisted of determining the antenna radiation patterns, voltage standing wave ratios (VSWR), and gain of both S-band and X-band antennas. The results were compared with the results obtained after thermal degradation of the test material.

The following procedure was used for making the real-time transmission-loss measurements. With the test model located as shown in figure 3, the recorders were adjusted to the desired levels without the arc jet operating. The recorder for the reflected power levels was calibrated by the use of short circuits and two calibrated attenuators. After all calibrations and adjustments were completed, the model was removed from the test position and the arc jet was ignited and adjusted to provide the proper test conditions. With all recording and monitoring equipment operating, the model was reinserted for the test. Each test was terminated when the temperature inside the model reached approximately 450° F (505° K). This maximum temperature was chosen to prevent damage to the aluminum substructure or antennas. Also, the adhesive bonding material used for attaching some of the test materials begins to lose strength rapidly at temperatures exceeding 450° F (505° K). The recording was continued after the arc jet was turned off until the measured transmission loss remained relatively constant.

After the model was removed from the arc jet, the measurements made prior to the thermal test were repeated to determine what effects thermal degradation of the ablation material had on the antenna characteristics.

RESULTS AND DISCUSSION

Electrical Properties

The dielectric properties of the test materials were measured at room temperature and the results are presented in table II. The test frequencies were determined by the

size of cavity used for holding the test material and by the dielectric constant of the material. Only one measurement of each material was made in the S-band to X-band frequency range since the dielectric constant for most good dielectrics does not change appreciably as a function of frequency.

Teflon and Plexiglas were measured to verify the accuracy of the measurement, which was within about 5 percent. All the materials measured have acceptable dielectric properties except Narmco 4028, which causes high losses because of its high carbon content. This material does not appear to be suitable for use as an antenna window.

The power transmission coefficients of all virgin materials were calculated (p. 35 of ref. 6) and are presented in table II. The calculations were made on the assumption that all materials had a thickness of $\lambda_\epsilon/2$, which would minimize losses due to mismatch.

Radiofrequency Transmission Loss in Arc Jet

The results of the transmission-loss measurements in the arc jet are presented in table III. Two loss values, designated as "hot" and "cold," are given for each model at each frequency. The values designated as hot are those obtained immediately after arc cutoff. The cold values are those obtained after the model had cooled until the recorded loss remained essentially constant. The values presented in table III indicate that the transmission loss for a given thickness of material does not vary linearly as a function of frequency. Figures 4 and 5 are typical transmission-loss recordings of the sequence of events during the thermal tests for two different materials at 2.66 GHz and 9.60 GHz.

No attempt was made to analyze the transmission-loss data obtained during the thermal test because of severe attenuation effects from the arc jet stream.

Antenna Radiation Patterns

The antenna radiation patterns of all models were measured before and after thermal degradation of the test material, using the coordinate system shown in figure 6. Some typical patterns for two of the models are presented in figures 7 and 8. One of the models was covered with cork and the other with Avcoat 5026-39 material. The cork caused low transmission losses after thermal degradation, which resulted in only minor changes in the antenna patterns (fig. 7), as is typical of low-loss materials. The Avcoat 5026-39 material produced very high transmission losses after thermal degradation and large perturbations in the antenna patterns (see figs. 8(b) and 8(d)).

These large pattern perturbations could also cause the real-time transmission-loss measurements (table III) to vary, depending on the exact location of the receiving

horn antenna in the measurement setup. For example, in figure 8(d) a variation of 10^{o} in elevation angle could result in a transmission-loss variation of 10 dB or greater. A variation of 10^{o} could easily have occurred because locations for mounting receiving antennas were limited by reflections from equipment such as arc-jet piping. However, care was taken to mount the models and receiving antennas in the same positions for all the tests.

In addition, the radiation patterns were measured several days after thermal degradation of the test materials, in which time the condition of the charred materials could have changed considerably and thus caused variations in the radiation patterns and gain measurements.

The severe charring of the phenolic-asbestos nose cap had no appreciable effects on the antenna patterns, as can be seen by comparing the before and after patterns in figures 7(b) and 7(d).

Voltage Standing Wave Ratios

Measurements of voltage standing wave ratio (VSWR) were made on all models before and after the thermal test. These measurements for two materials, cork and Avcoat 5026-39, are given in figure 9. The VSWR for the cork material (fig. 9(a)) did not change appreciably after the material was subjected to the thermal test; however, the VSWR for the Avcoat 5026-39 material (fig. 9(b)) increased considerably. This increase in VSWR accounts for less than 2 dB of the total transmission loss, which varied from 16.5 dB to 45 dB for the Avcoat 5026-39 material.

The VSWR's for all materials, except Narmco 4028 both before and after thermal exposure, were less than 4. However, as was stated previously, even in its virgin state this material is not acceptable as an antenna cover or window because of its high transmission loss (>30 dB).

It is interesting to note that the VSWR levels observed during the arc-jet tests were very small for all materials except Narmco 4028, even though a conductive char was developed on some of the test materials.

Description of Models After Thermal Test

Photographs of the models after they were subjected to the thermal test are shown in figure 10. In this section the irregularities that could cause errors in measurement of the antenna characteristics of some models are described.

Figure 10(a) shows the Avcoat II model, which is partially covered with a residue that resembles soot in both color and texture. The cork-covered model is shown in figure 10(b). Almost all the test material was consumed during the thermal test, and

that which remained had the appearance of a wood char. The Avcoat 5026-39 model is shown in figure 10(c). A deposit of glass was left on the upper portion of the model, apparently from the erosion of the phenolic-asbestos nose cap. The test material appeared to be charred to the bond line. Figure 10(d) shows the E4A1 test model, on which a low-density phenolic-nylon nose cap was used. Immediately after the thermal test began, large cracks developed in the test material; however, as the test continued the cracks appeared to close up somewhat until they reached the condition shown in the photograph at the end of the test. Some of these cracks occurred over the test antennas. In addition, this model had to be handled with extreme care to permit measurement of the antenna characteristics after the thermal test because the material appeared to be separating from the substructure at the bond line and was very fragile. Figure 10(e) shows the Narmco 4032C material which developed many small surface cracks during the thermal test. The phenolic-nylon model (fig. 10(f)) shows the type of carbonaceous char layer formed during the ablation of this type of material. The material appeared to be charred completely to the bond line and the nose cap was fused to the substructure and had to be sawed off to allow removal of the test antennas. A considerable amount of material had fallen off the model, making measurement of the antenna characteristics difficult. Figure 10(g) shows the Narmco 4028 material, which, like the Narmco 4032C material, developed many small surface cracks during the thermal test.

Transmission Losses Determined From Antenna Gain Measurements

The transmission-loss values obtained from the antenna gain measurements are presented in table IV. These values were obtained by finding the differences between the absolute gain values measured before and after thermal degradation of each ablation material. (The gain values were determined by comparison with a reference antenna.) The gain values measured after the thermal test were subject to the following conditions:

(a) Perturbations of antenna radiation patterns

(b) VSWR variations

(c) Physical condition and aging of test material

An example was presented previously of a material (Avcoat 5026-39) that produced severe perturbations in the radiation patterns after thermal degradation which could have caused errors in the transmission-loss measurements given in table IV. Narmco 4028 was the only material that had a VSWR loss of more than 2 dB after thermal degradation. The physical condition of the E4A1 and phenolic-nylon models had a very definite effect on the transmission-loss measurements presented in table IV. For some of the models of these two materials, the values given in table IV differ greatly from the cold-loss values in table III. These differences are attributed to cracks in the test material, loss

of charred material over the antenna apertures after thermal exposure, and possible changes due to aging of the charred material, since these measurements were made a few weeks after the thermal test was conducted.

CONCLUDING REMARKS

The transmission loss, radiation-pattern perturbations, and VSWR changes of typical antennas, produced by thermally degraded ablation materials, have been investigated experimentally. Dielectric constants and loss tangents of the test materials were measured at room temperature. All the materials had acceptable dielectric properties except Narmco 4028, which had a very high loss tangent due to its high carbon content and therefore was considered unsuitable as an antenna window or cover.

The transmission losses through several thermal protection materials measured at 2.66 GHz and 9.60 GHz in a high-energy arc-heated airstream indicated that, in general, materials which form and retain appreciable conductive char layers during thermal exposure produce very high transmission losses. A typical material of this type is Avcoat 5026-39.

Measurements of antenna radiation patterns after thermal degradation indicated that a material which produced high transmission losses may also produce perturbations in the radiation patterns of the antenna which it is covering. Low-loss materials, however, produced only slight changes in the antenna patterns after thermal exposure.

The VSWR of the antennas increased when a high-loss material was covering them; however, this VSWR mismatch of less than 4 contributed less than 2 dB to the total transmission-loss values presented.

Measurements of transmission losses through the thermally degraded test materials after the model has been removed from the arc jet are subject to changes in the physical condition of the test material and also any changes in the char characteristics produced by aging.

Langley Research Center,
National Aeronautics and Space Administration,
Langley Station, Hampton, Va., May 20, 1968,
125-22-02-02-23.

REFERENCES

1. Dow, Marvin B.; Pittman, Claud M.; and Croswell, William F.: Thermal Performance and Radio-Frequency Transmissivity of Several Ablation Materials. NASA TN D-1896, 1964.

2. Croswell, William F.: Antennas Under Ablation Materials. Conference on Langley Research Related to Apollo Mission, NASA SP-101, 1965, pp. 239-265.

3. Altschuler, H. M.: Dielectric Constant. Handbook of Microwave Measurements, Third Ed., Vol. II, Max Sucher and Jerome Fox, eds., Polytech. Press of Polytech. Inst. Brooklyn, 1963, pp. 495-548.

4. Ginzton, Edward L.: Microwave Measurements. McGraw-Hill Book Co., Inc., 1957.

5. Chapman, Andrew J.: An Experimental Evaluation of Three Types of Thermal Protection Materials at Moderate Heating Rates and High Total Heat Loads. NASA TN D-1814, 1963.

6. Tice, Thomas E., ed.: Techniques for Airborne Radome Design. WADC Tech. Rept. 57-67, ASTIA Doc. No. AD 142001, U.S. Air Force, Sept. 1957.

TABLE I

TEST-MATERIAL CHARACTERISTICS

Test material	Test-material composition	Bond material	Test-material thickness			
			t		t_s	t_x
			in.	cm		
Avcoat II	Epoxy and additives	Self-bonding	0.25	0.635	0.092	0.332
Cork	Cork and phenolic binder	Epoxy and fillers	.25	.635	.076	.272
Avcoat 5026-39	Avco 5026-39 gunned into nylon-phenolic 3/8-in. (1-cm) honeycomb	Epoxy and fillers	.25	.635	.085	.305
E4A1 (developed at Langley Research Center)	Silicone elastomer with fillers	GE RTV-60	.25	.635	.081	.291
Phenolic nylon	50 percent phenolic and 50 percent nylon (by weight)	Epoxy and fillers	.25	.635	.105	.376
Narmco 4028	Modified phenolic reinforced with carbon fibers	Epoxy and fillers	.25	.635	.083	.298
Narmco 4032C	Nylon-phenolic resin with high-silica fibers	Epoxy and fillers	.25	.635	.103	.372

TABLE II

ELECTRICAL PROPERTIES OF ABLATION MATERIALS AT ROOM TEMPERATURE

Material	Frequency, GHz	Dielectric constant, ϵ_r	Loss tangent, tan δ	Power transmission coefficient, $\lvert T \rvert^2$
Teflon	10.03	2.00	0.0007	0.998
Plexiglas	8.84	2.57	.0045	.984
Avcoat II	6.14	2.68	.013	.954
Cork	9.87	1.80	.050	.835
Avcoat 5026-39:				
With grain	9.82	2.26	.031	.894
Cross grain	9.82	2.25	.035	.881
E4A1	9.63	2.16	.013	.956
Phenolic nylon	5.46	3.36	.018	.933
Narmco 4028	9.92	2.05	.200	$\approx$.500
Narmco 4032C	7.64	3.44	.011	.959

TABLE III

RADIOFREQUENCY TRANSMISSION LOSSES DUE TO CHAR MEASURED IN ARC JET

Test material	Test specimen	Transmission loss, dB, at 2.66 GHz		Transmission loss, dB, at 9.60 GHz		Test time, sec
		Hot	Cold	Hot	Cold	
Avcoat II	1	1	1	5	2.0	11.5
	2	3.4	1.2	5.4	2.0	19.5
Cork	1	5	1	7.6	2.4	53
	2	5.6	1.2	14	3.5	54
Avcoat 5026-39	1	20	16.8	41	37	50
	2	21	16.5	24.6	23.4	57
	3	26	20.6	44	45	55
	4	20.2	17.6	42	38	55
E4A1	1	21	16	47.2	27.2	95
	2	26.5	22.5	20	13.4	89
	3	19.8	15.6	38	34	90
	4	16.8	16.2	32	31.2	90
Phenolic nylon	1	18	20.2	22	24.2	103
	2	14	15	17	20.2	90
Narmco 4028[a]	1	15	-7	7	0	44
	2	[b]10	[b]9	[b]3.2	[b]2.8	44, 28
Narmco 4032C	1	18.2	27.4	25.5	27.4	83

[a]Radiofrequency transmission loss through virgin material was greater than 30 dB and the numbers given here represent the additional loss (or, in the case of a negative number, the decrease in loss) after charring.

[b]Model was exposed to thermal test twice with total time of 72 seconds.

TABLE IV

RADIOFREQUENCY TRANSMISSION LOSSES DUE TO CHAR DETERMINED FROM ANTENNA GAIN

Test material	Test specimen	Loss, dB, at –	
		2.66 GHz	9.60 GHz
Avcoat II	1	1	1.2
	2	1	1
Cork	1	1	1
	2	1	4.0
Avcoat 5026-39	1	30	36.8
	2	28.4	28.8
	3	21.8	[a]22.2
	4	20.8	25.6
E4A1	1	26.3	29
	2	23.6	31.7
	3	[b]12.4	27.4
	4	7.4	22.6
Phenolic nylon	1	17	9.1
	2	[c]10.6	(d)
Narmco 4028	1	(e)	(e)
Narmco 4032C	1	23.4	32.4

[a]Loss value is dependent on angle chosen for gain value on antenna pattern because of severe deterioration of pattern.

[b]Material buckled and cracked over S-band antenna.

[c]Considerable amount of charred material had fallen off model; therefore, attenuation values are reduced.

[d]No value available.

[e]Losses through virgin material were greater than 30 dB and no significant change was measured after charring.

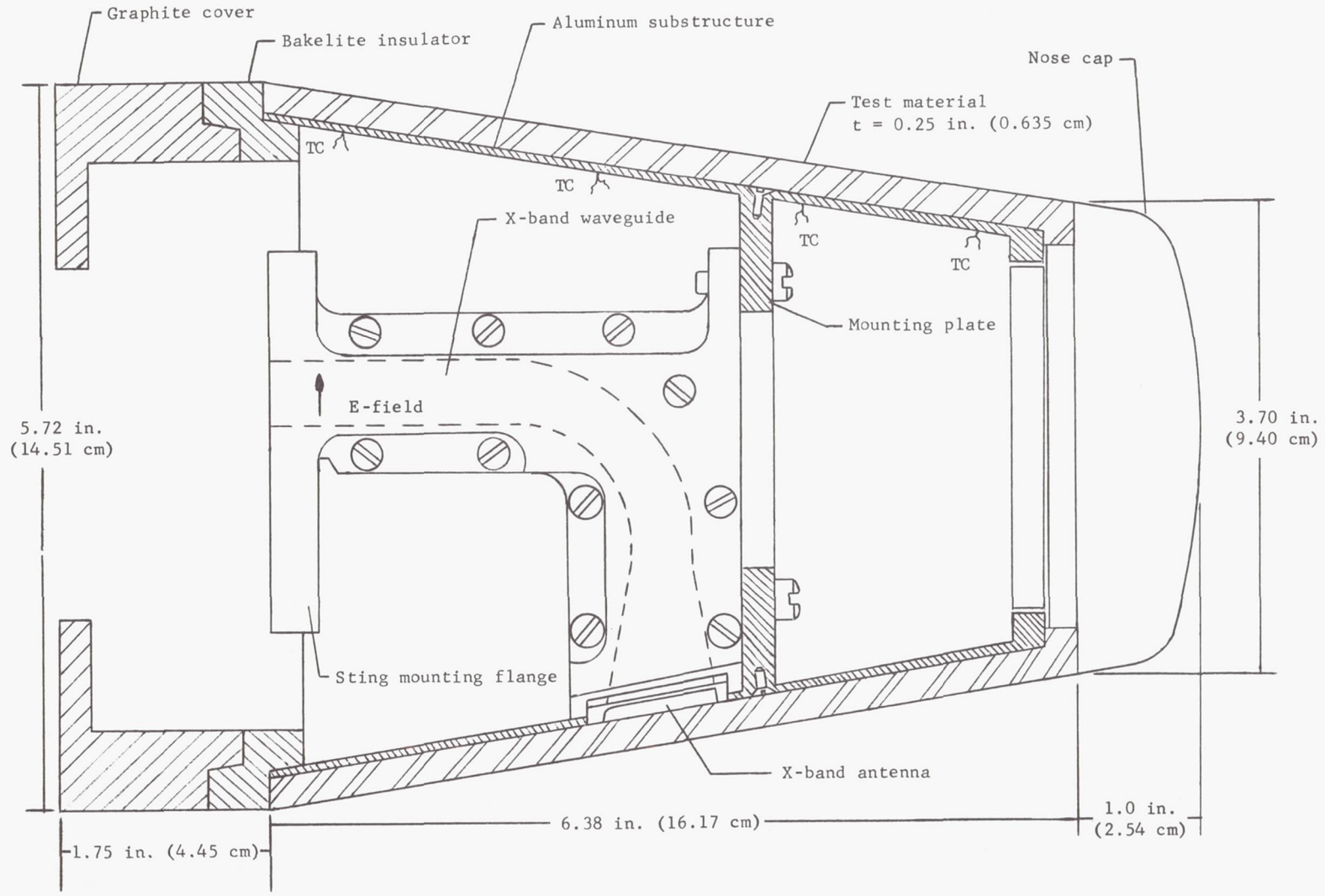

(a) View showing X-band antenna.

Figure 1.- Model configuration.

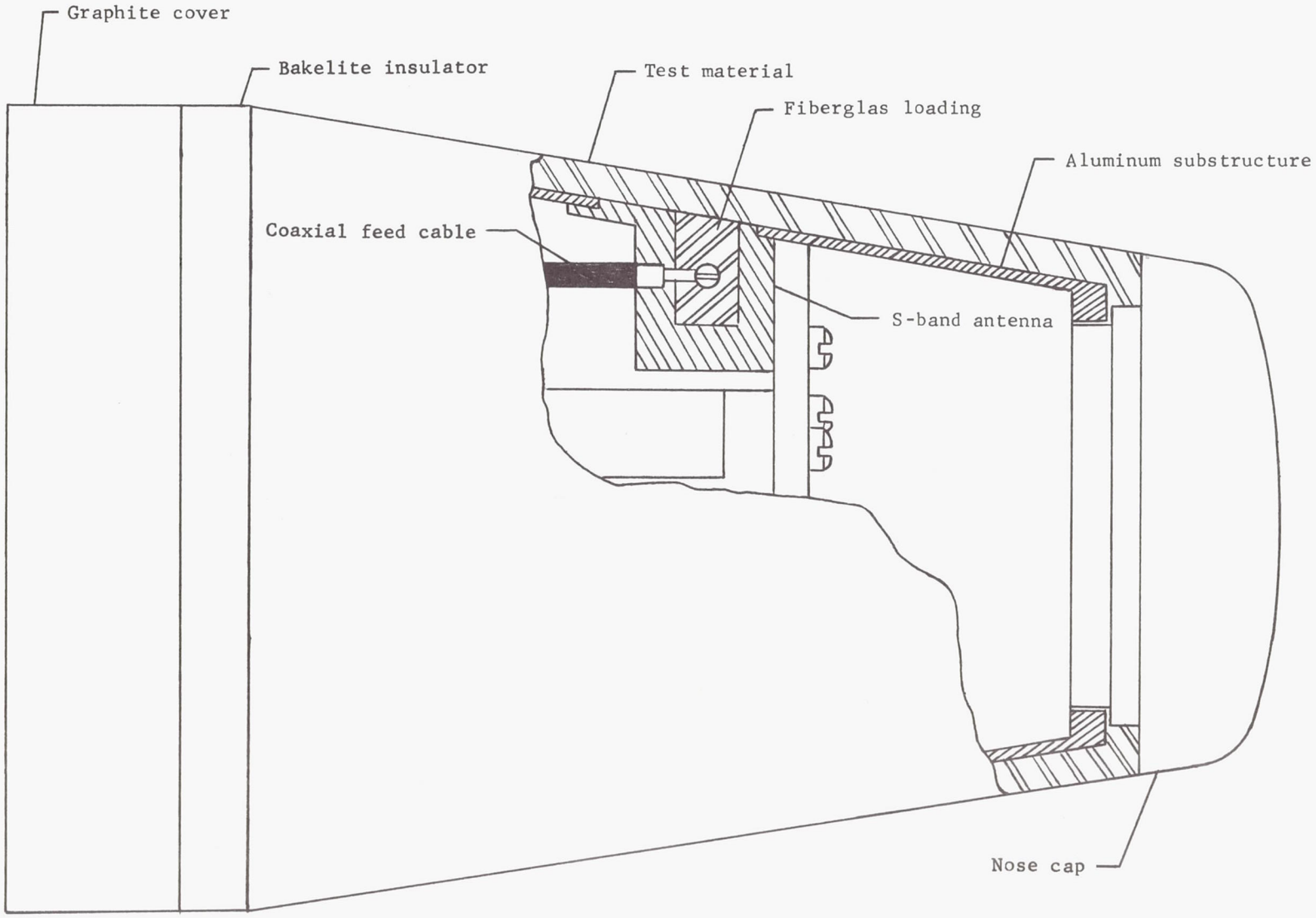

(b) View showing S-band antenna.

Figure 1.- Concluded.

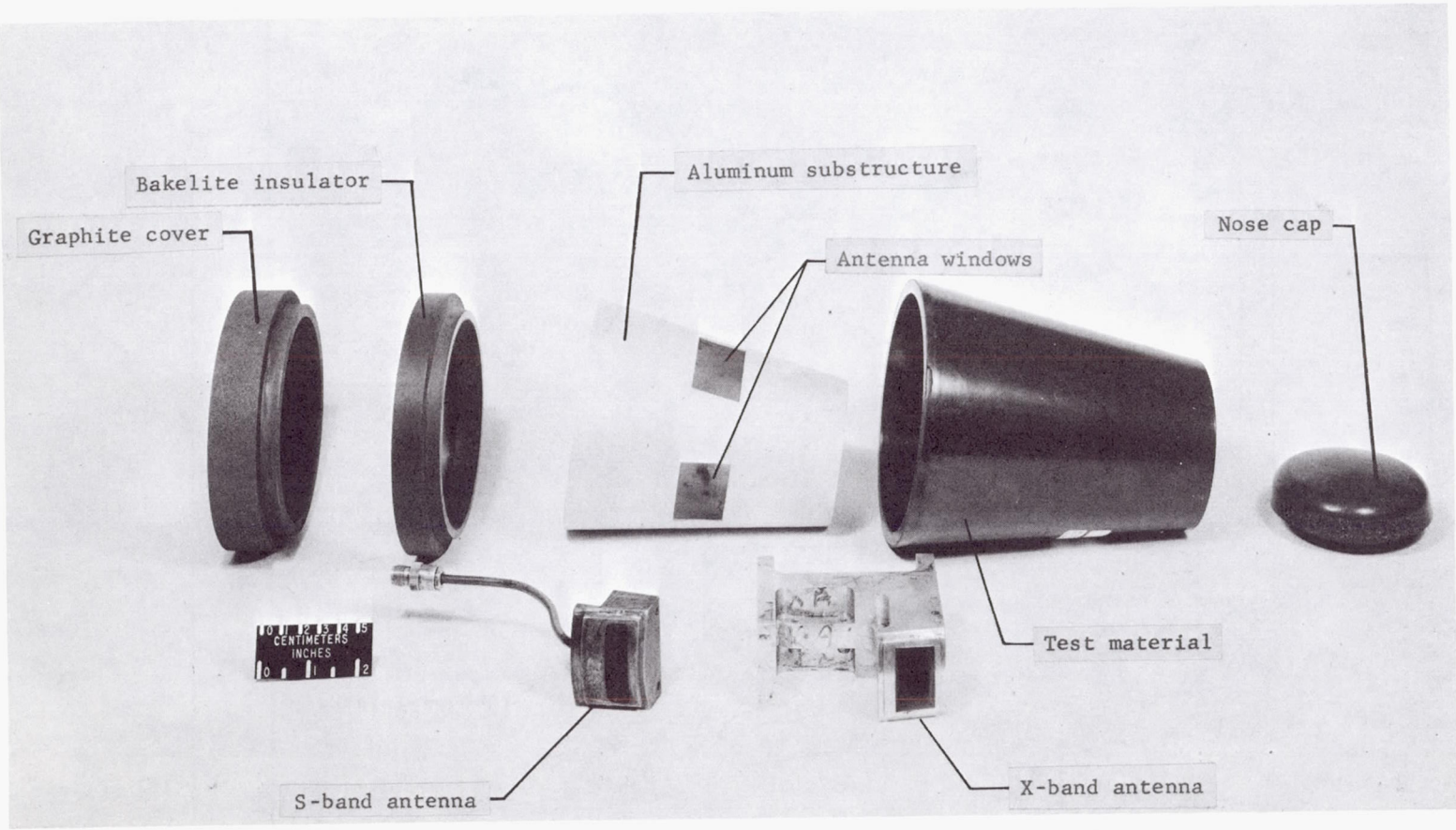

Figure 2.- Components of models.

L-66-6574.1

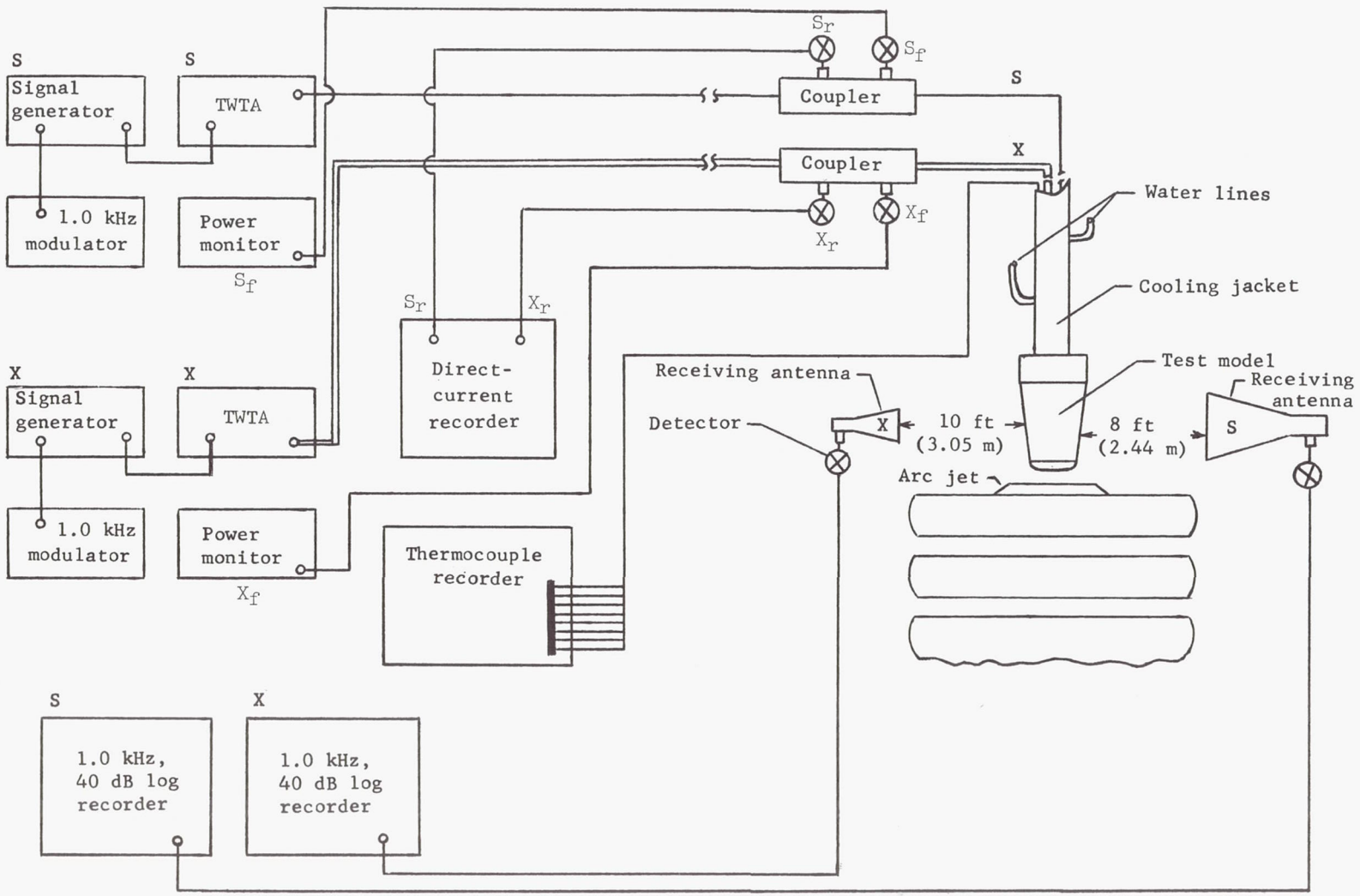

Figure 3.- Block diagram of setup for transmission-loss measurement in arc jet.

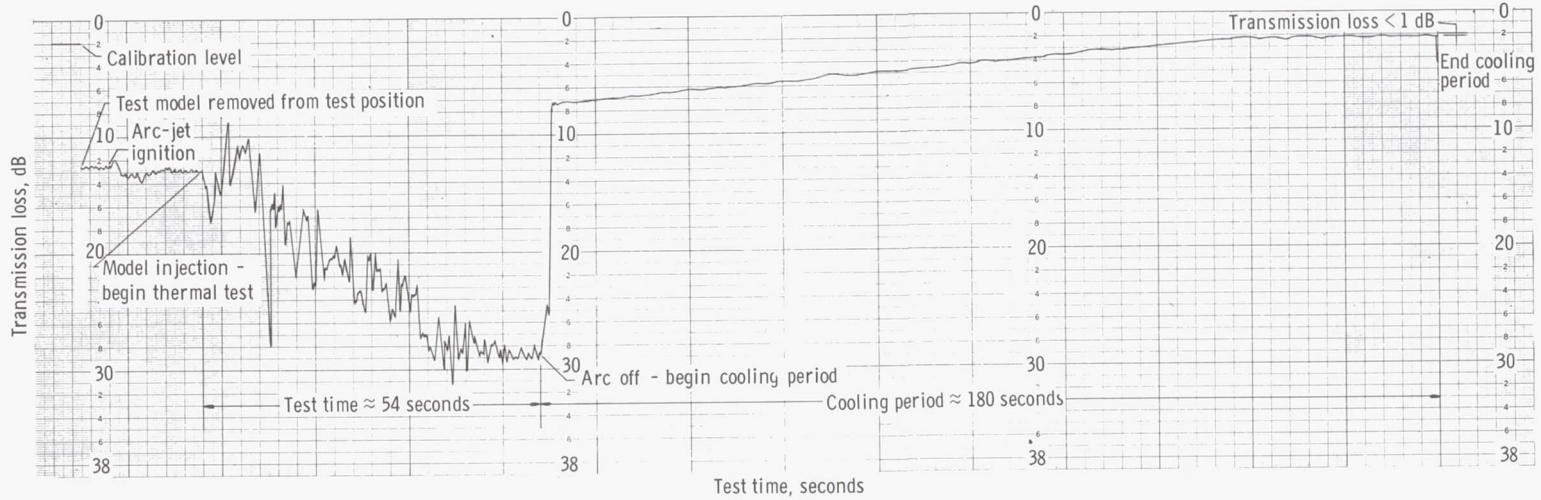

(a) Frequency of 2.66 GHz.

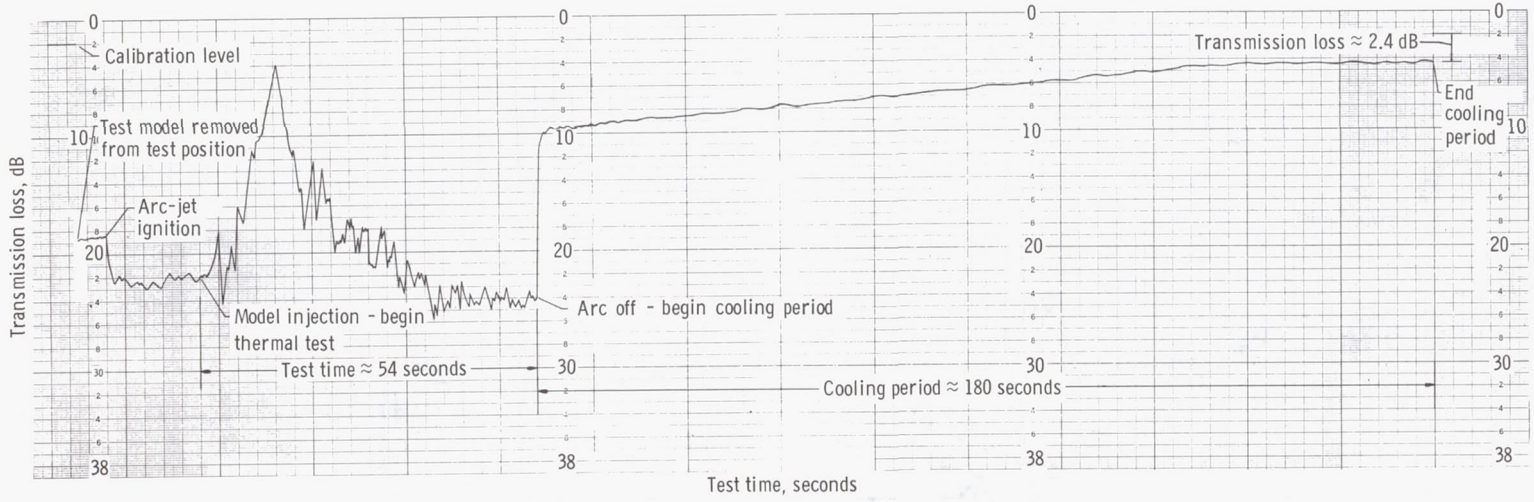

(b) Frequency of 9.60 GHz.

Figure 4.- Transmission-loss recording during thermal test in arc jet for cork.

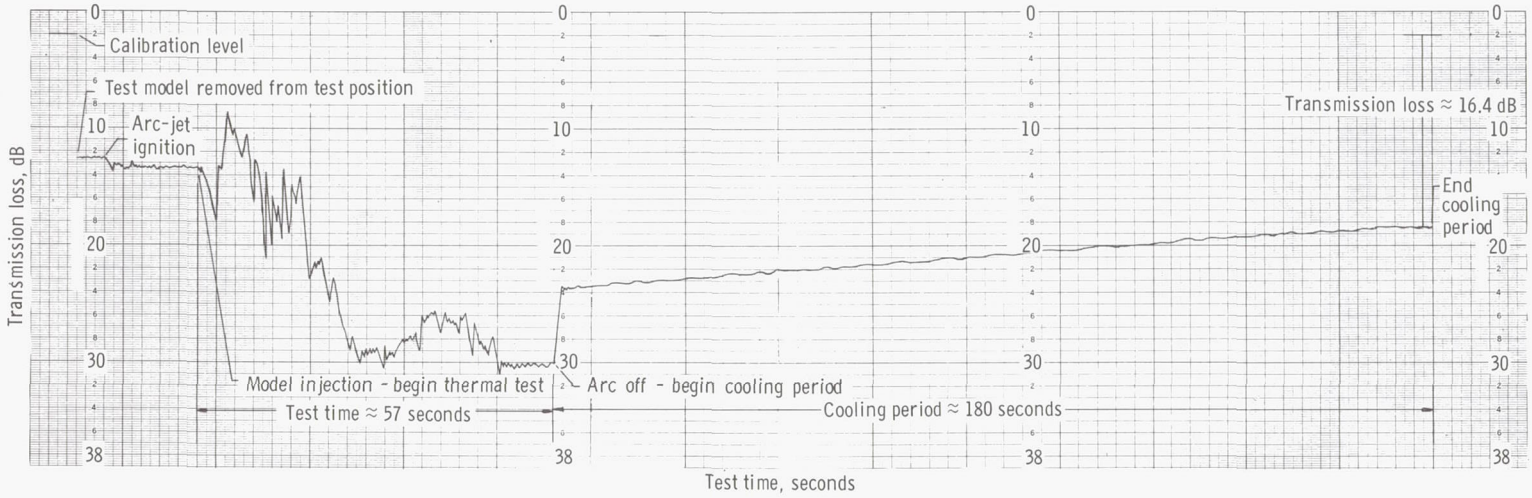

(a) Frequency of 2.66 GHz.

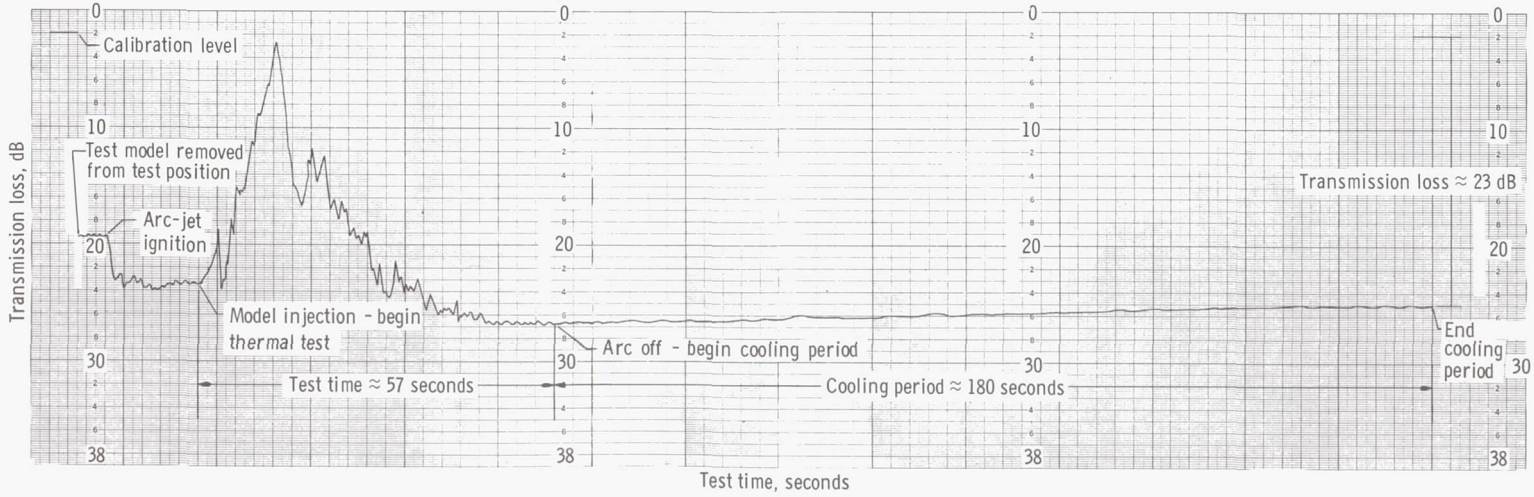

(b) Frequency of 9.60 GHz.

Figure 5.- Transmission-loss recording during thermal test in arc jet for Avcoat 5026-39.

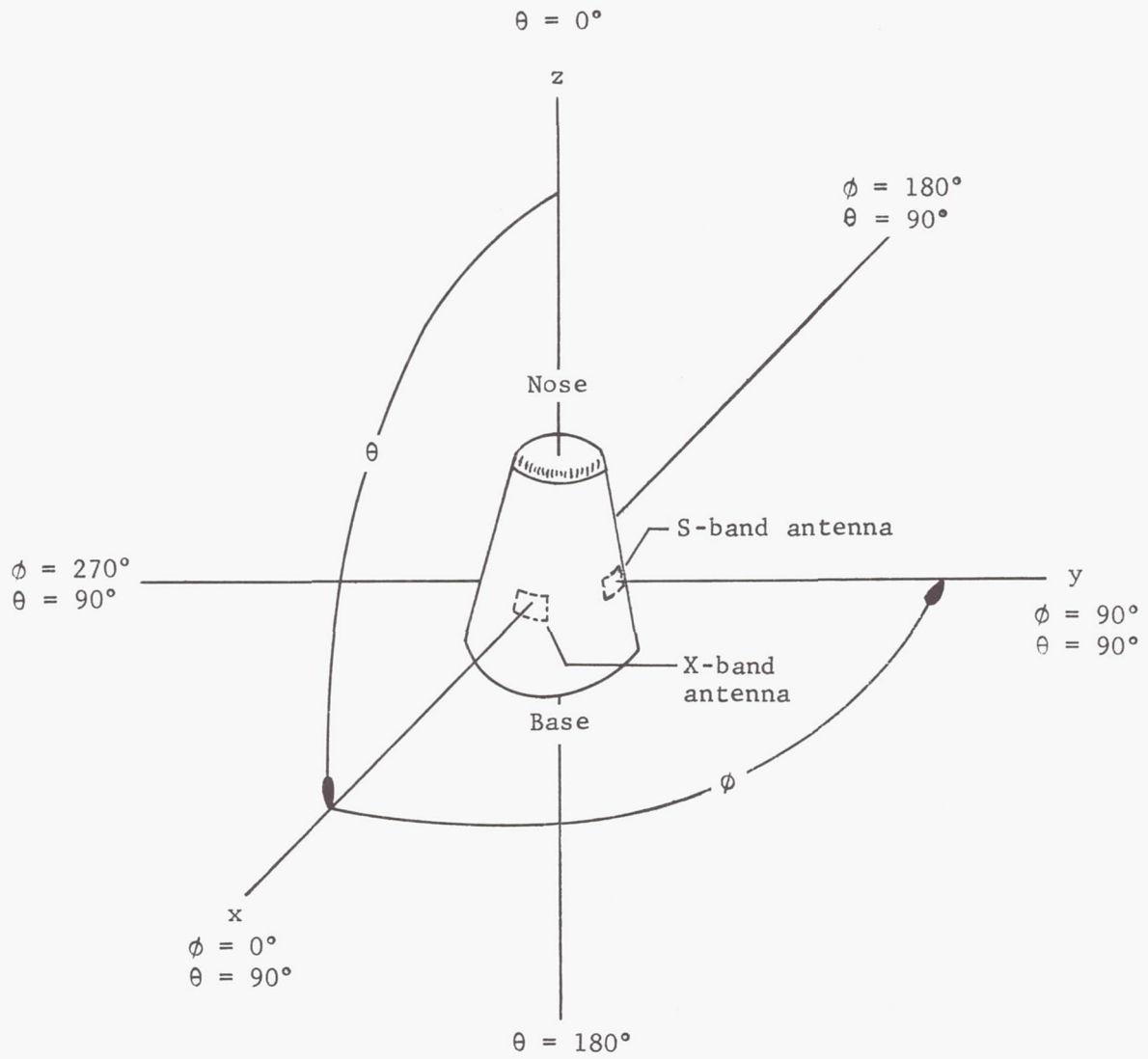

Figure 6.- Geometry of test-model antenna patterns.

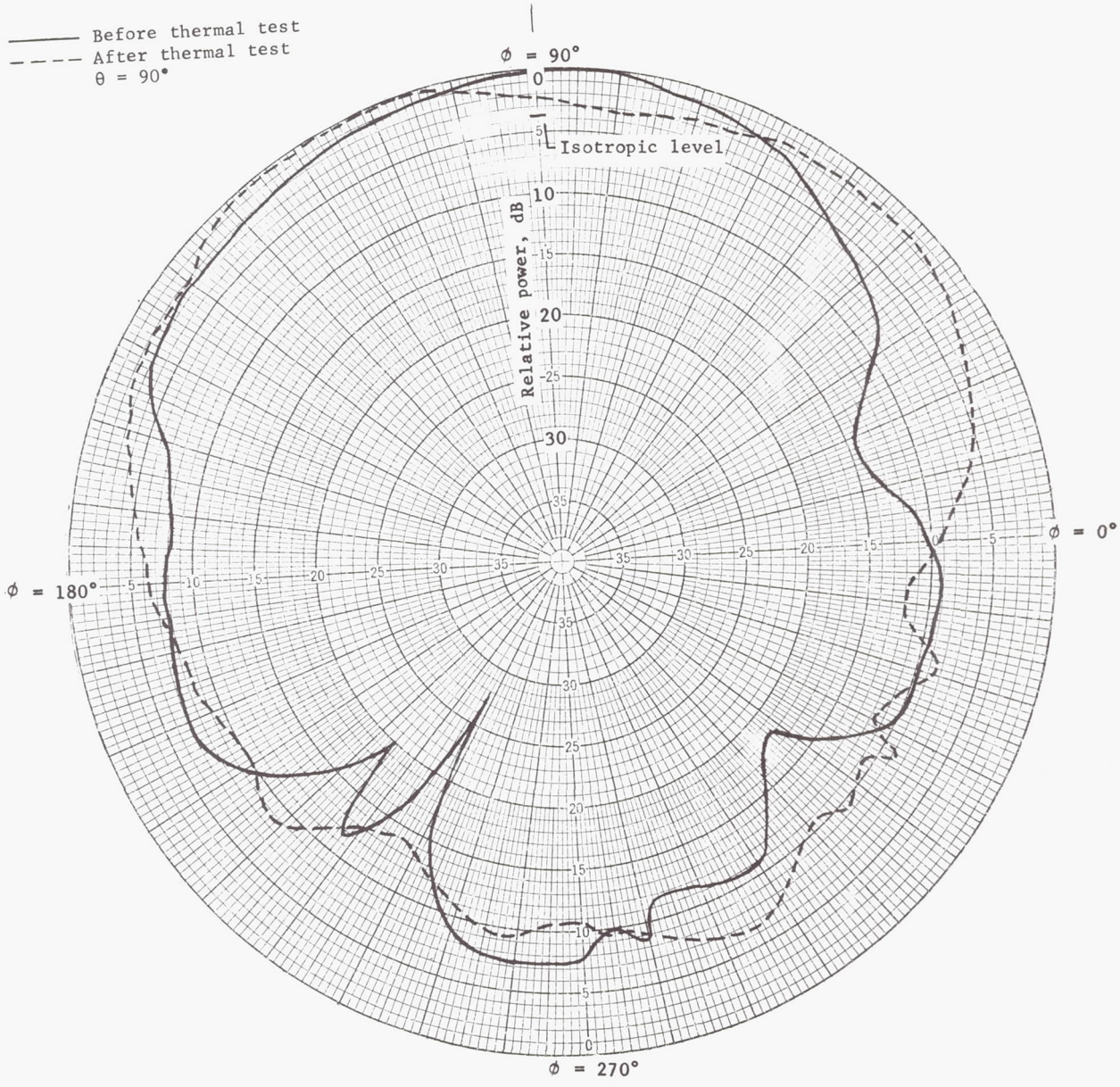

(a) Frequency, 2.66 GHz; H-plane pattern; antenna located at $\theta = 90^{0}$, $\Phi = 90^{0}$.

Figure 7.- Typical antenna radiation patterns for cork.

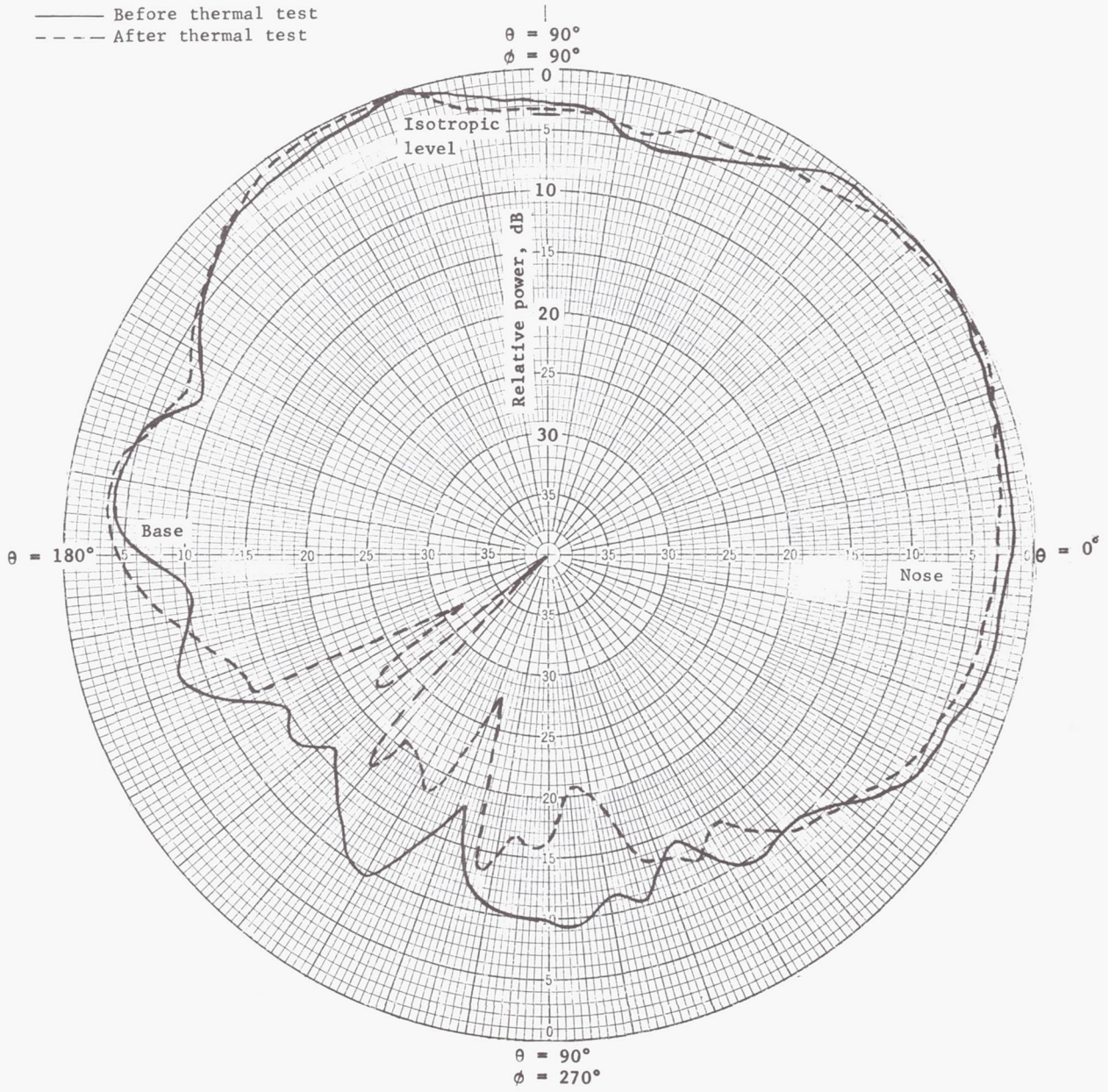

(b) Frequency, 2.66 GHz; E-plane pattern; antenna located at $\theta = 90^{0}$, $\Phi = 90^{0}$.

Figure 7.- Continued.

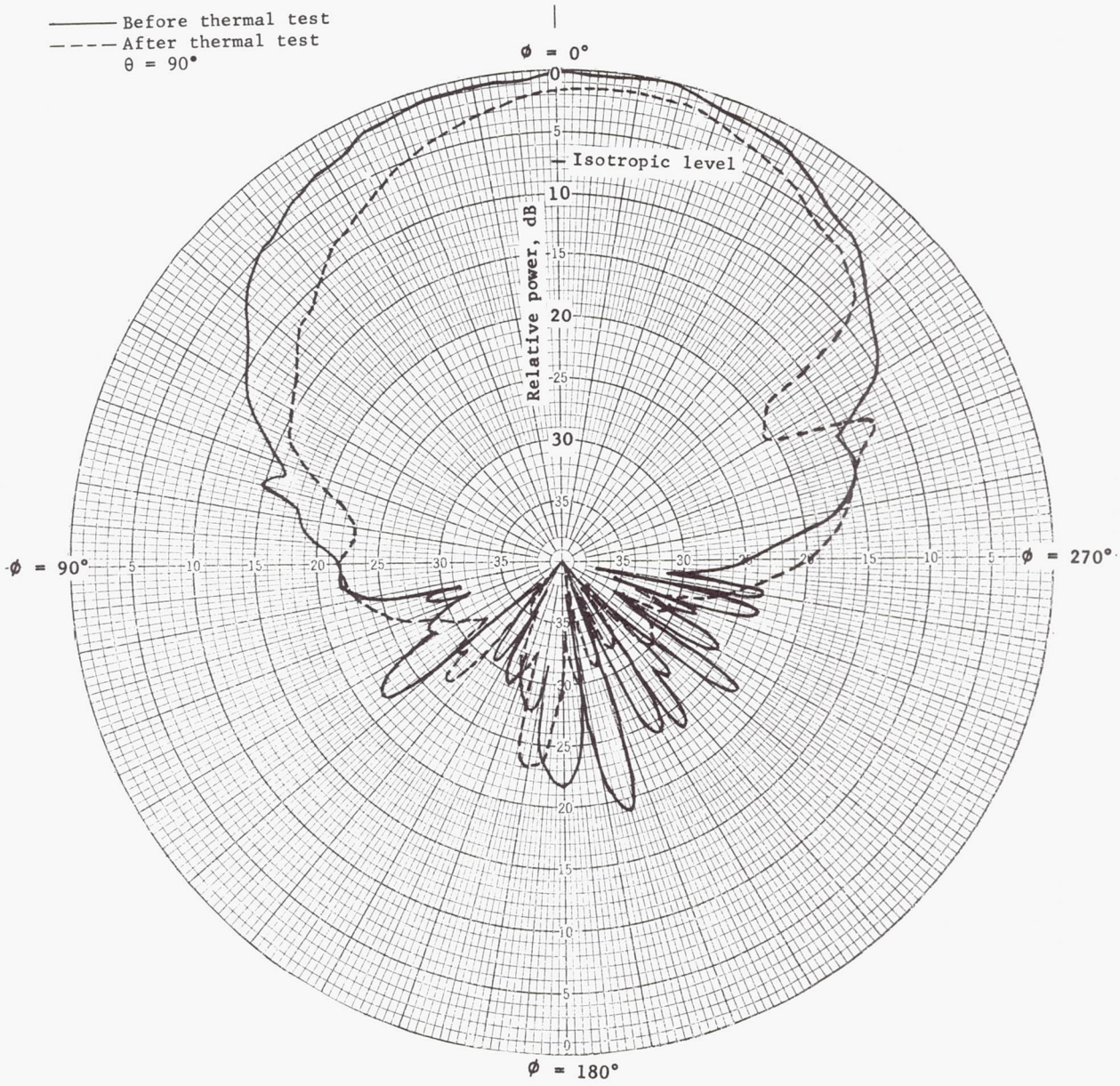

(c) Frequency, 9.60 GHz; H-plane pattern; antenna located at $\theta = 90^{o}$, $\Phi = 0^{o}$.

Figure 7.- Continued.

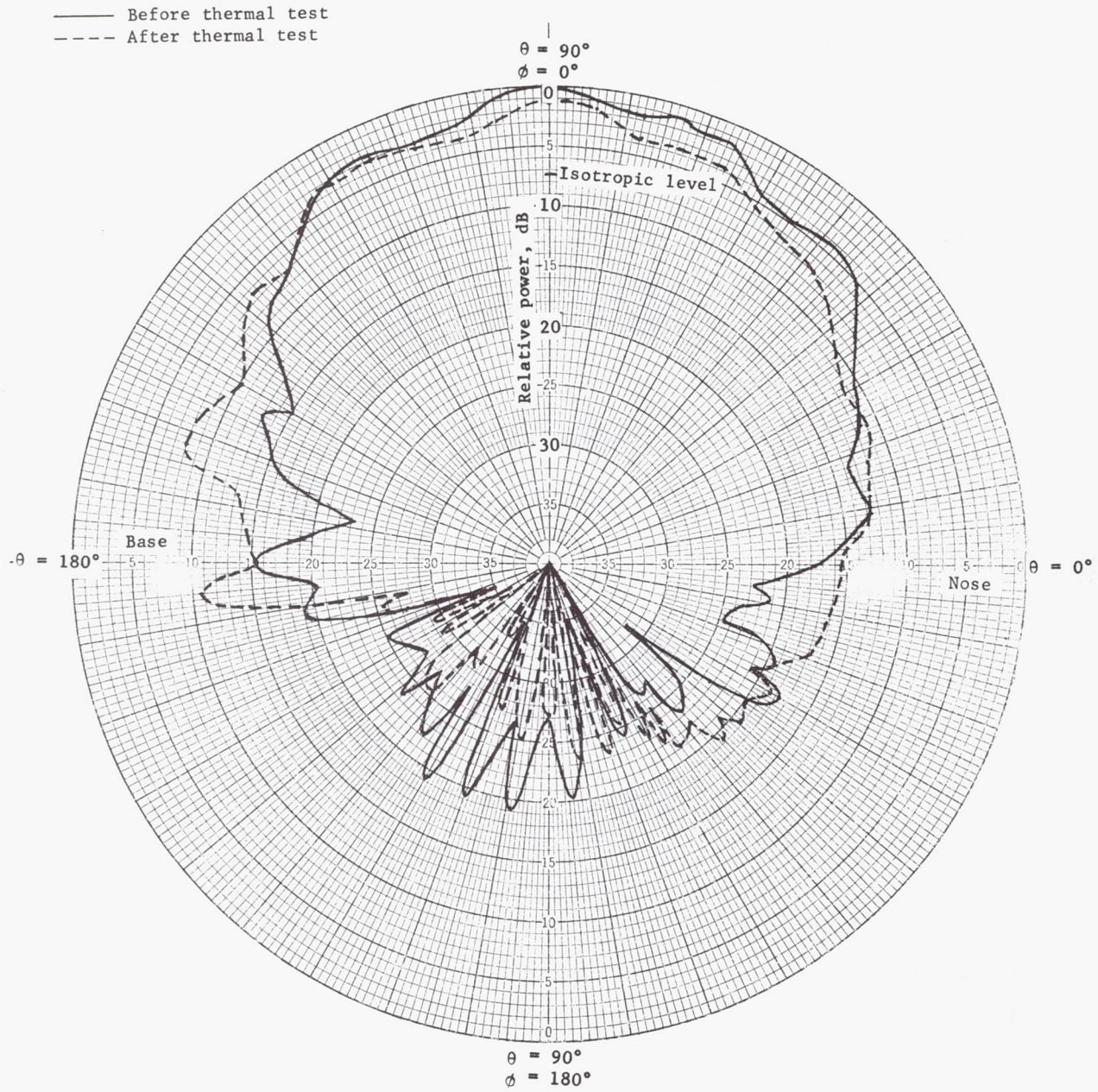

(d) Frequency, 9.60 GHz; E-plane pattern; antenna located at $\theta = 90^{0}$, $\Phi = 0^{0}$.

Figure 7.- Concluded.

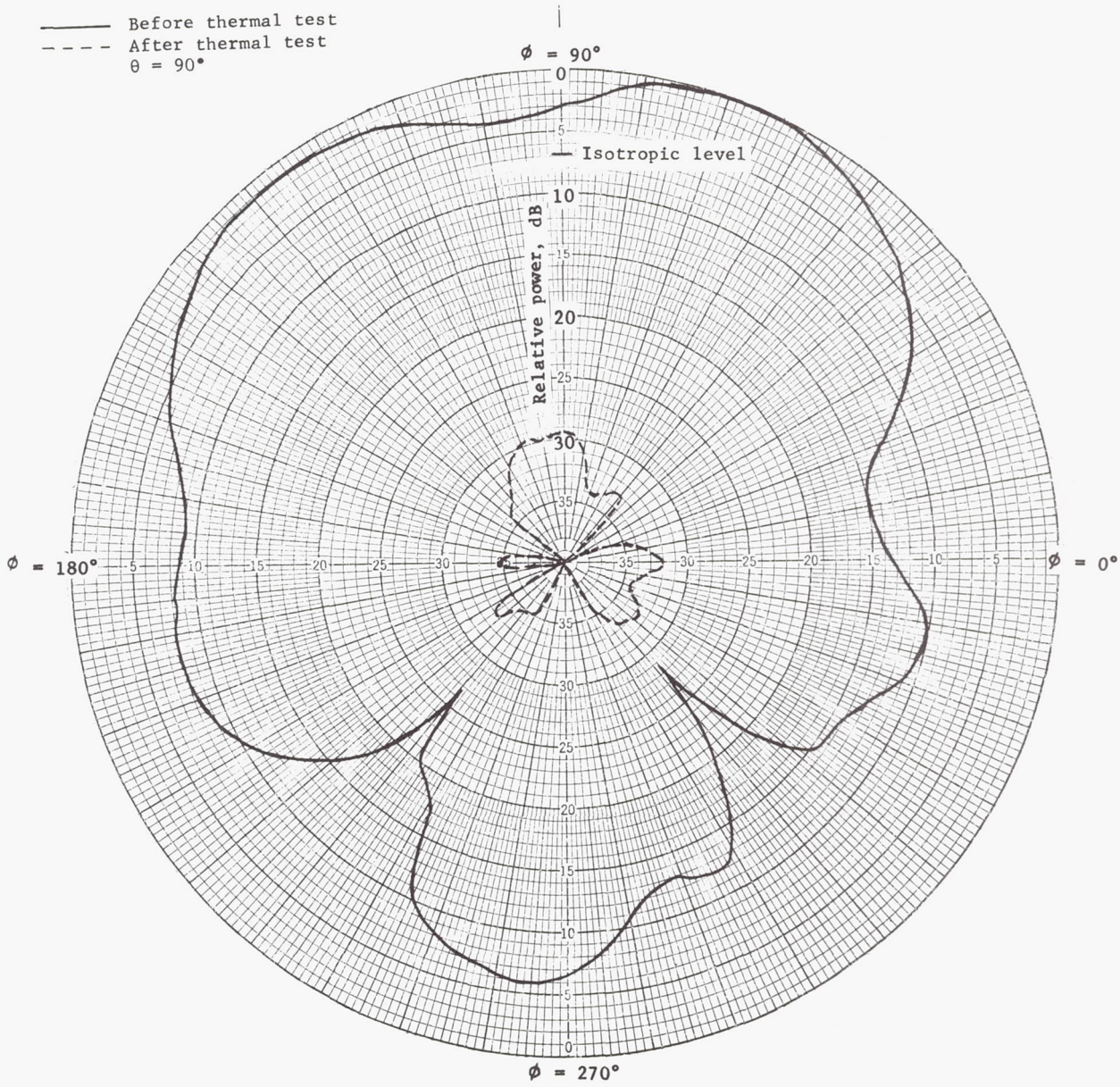

(a) Frequency, 2.66 GHz; H-plane pattern; antenna located at $\theta = 90^0$, $\Phi = 90^0$.

Figure 8.- Typical antenna radiation patterns for Avcoat 5026-39.

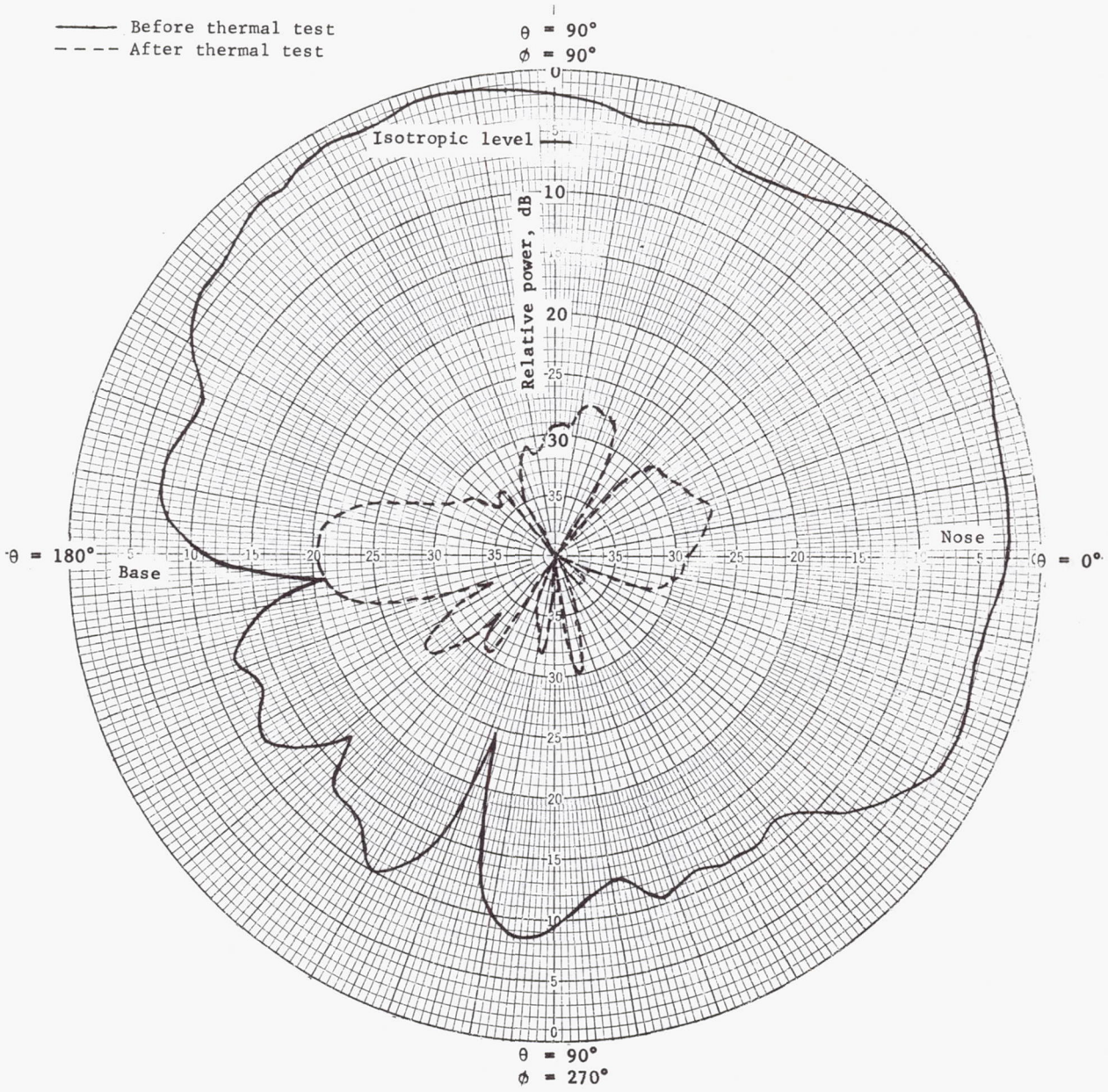

(b) Frequency, 2.66 GHz; E-plane pattern; antenna located at $\theta = 90^0$, $\Phi = 90^0$.

Figure 8.- Continued.

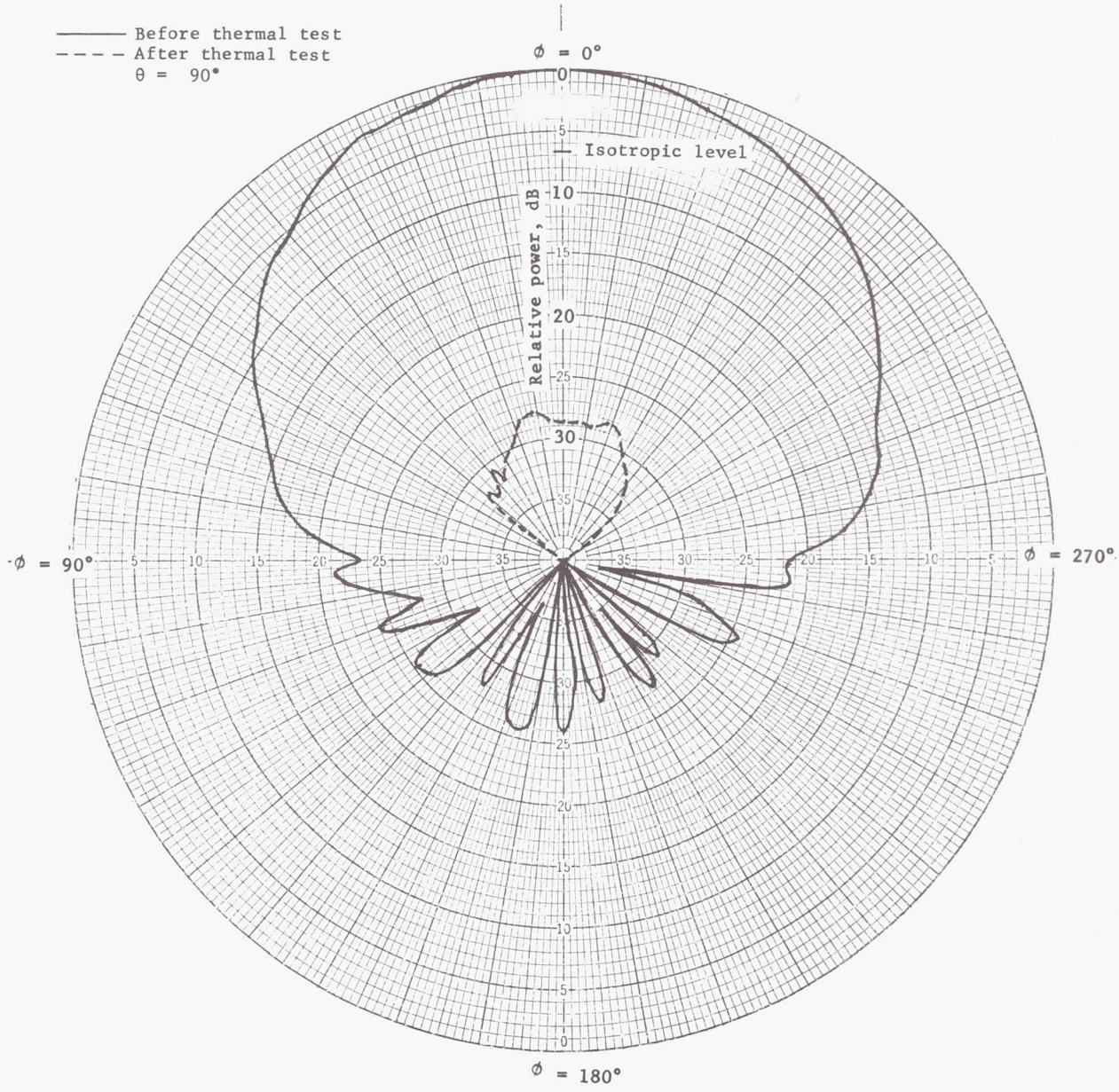

(c) Frequency, 9.60 GHz; H-plane pattern; antenna located at $\theta = 90^0$, $\Phi = 0^0$.

Figure 8.- Continued.

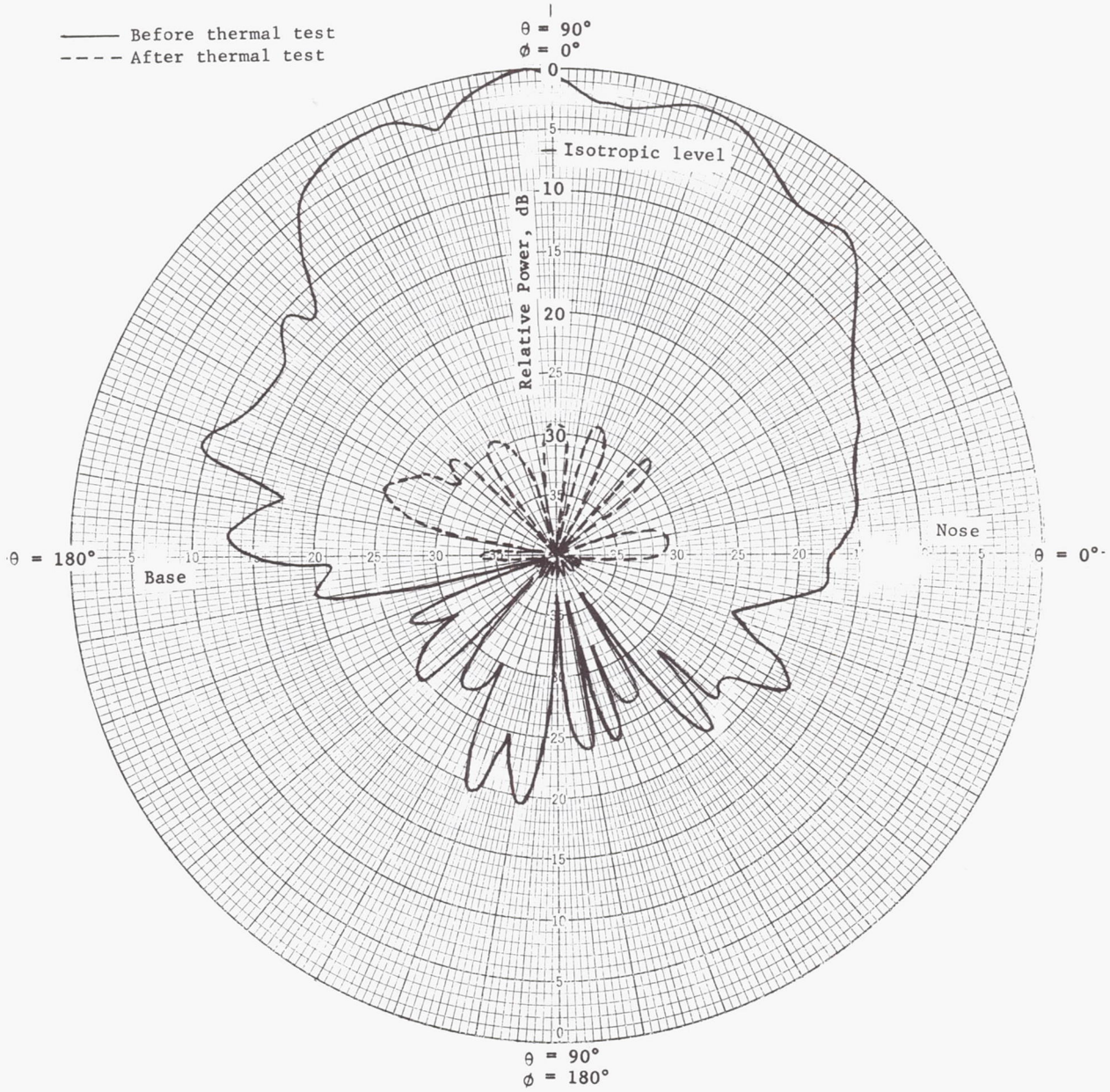

(d) Frequency, 9.60 GHz; E-plane pattern; antenna located at $\theta = 90^0$, $\phi = 0^0$.

Figure 8.- Concluded.

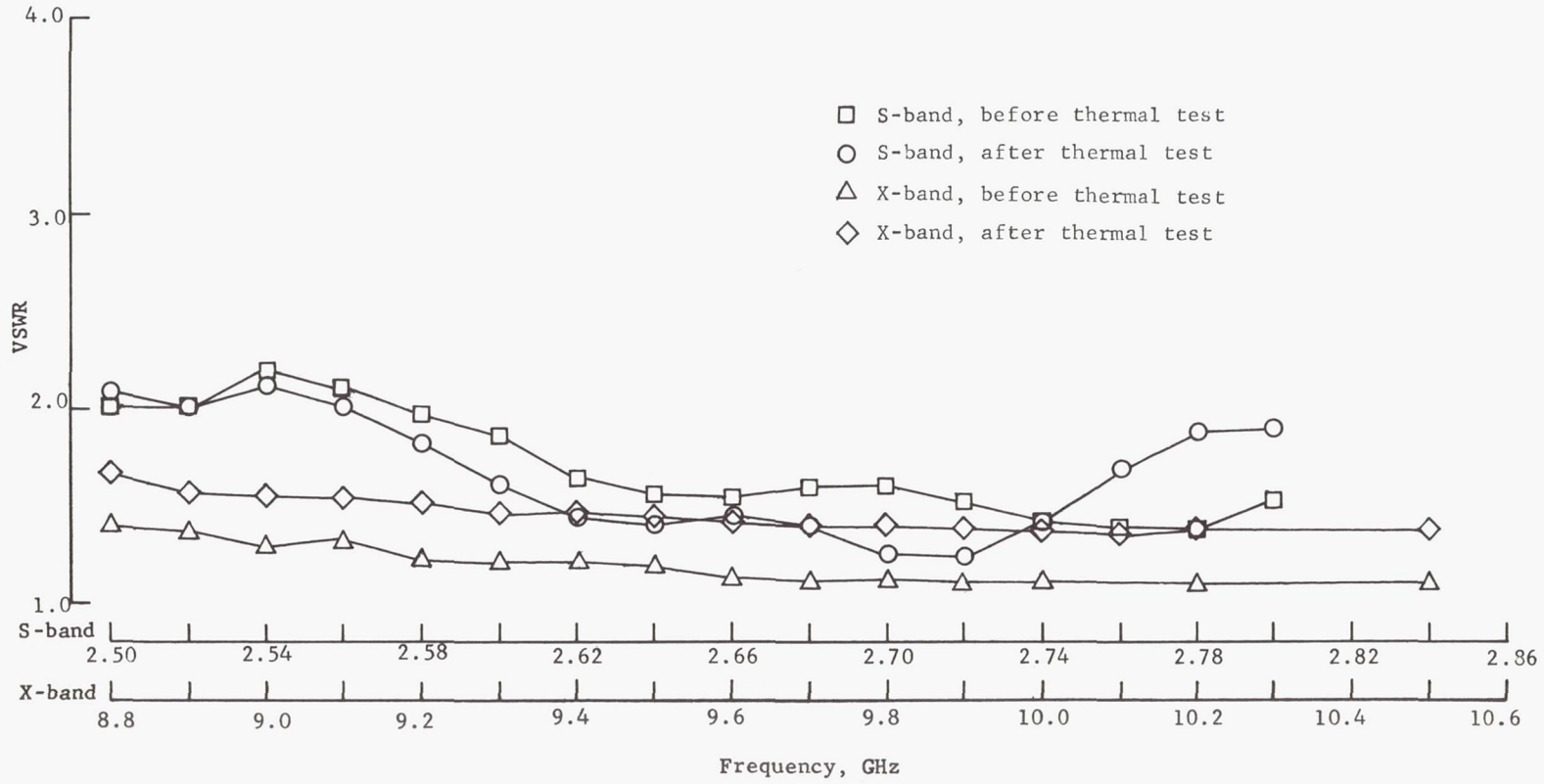

(a) Cork.

Figure 9.- Antenna voltage standing wave ratio (VSWR) as a function of frequency before and after thermal test.

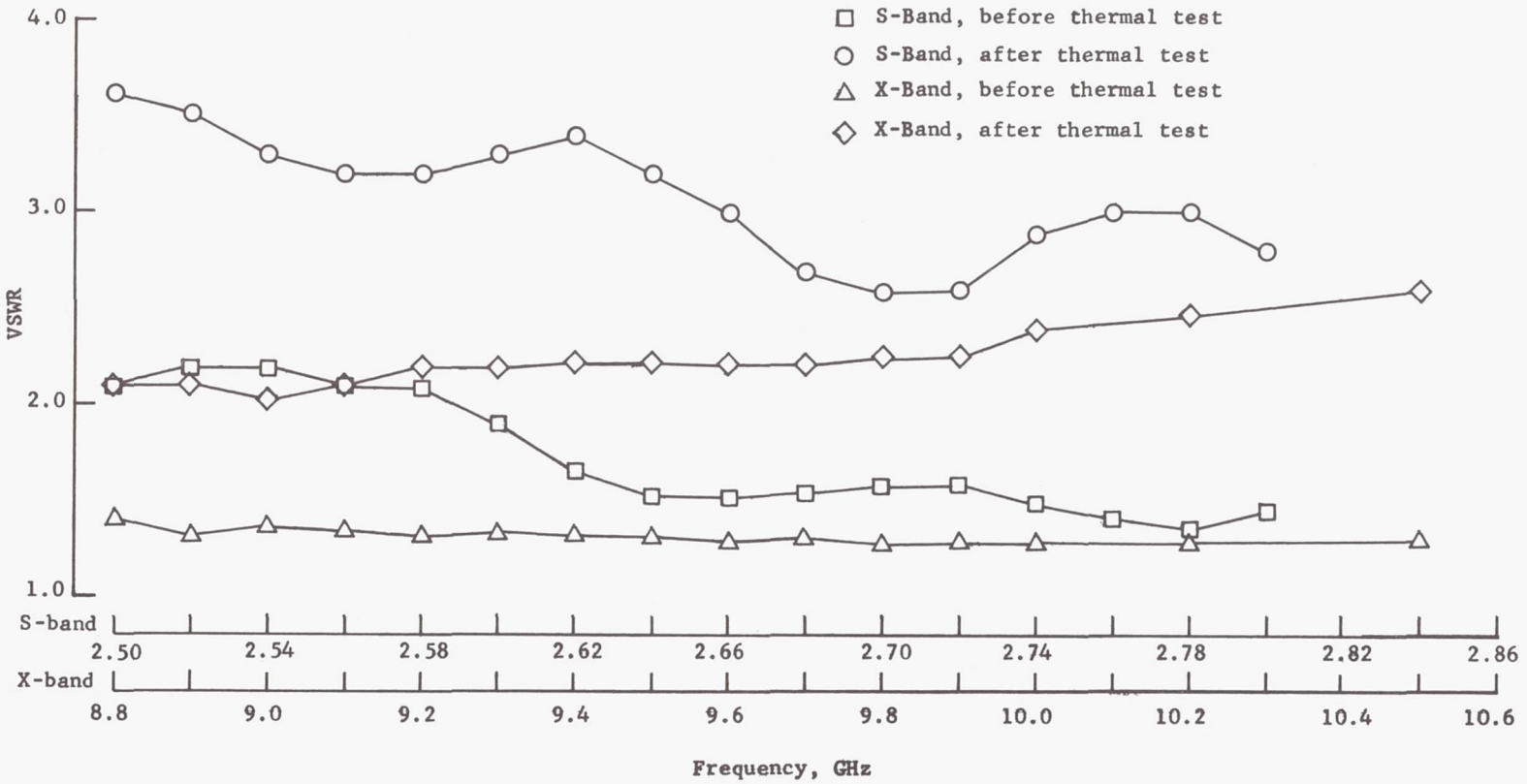

(b) Avcoat 5026-39.

Figure 9.- Concluded.

(a) Avcoat 11.

L-66-2561

Figure 10.- Models after testing.

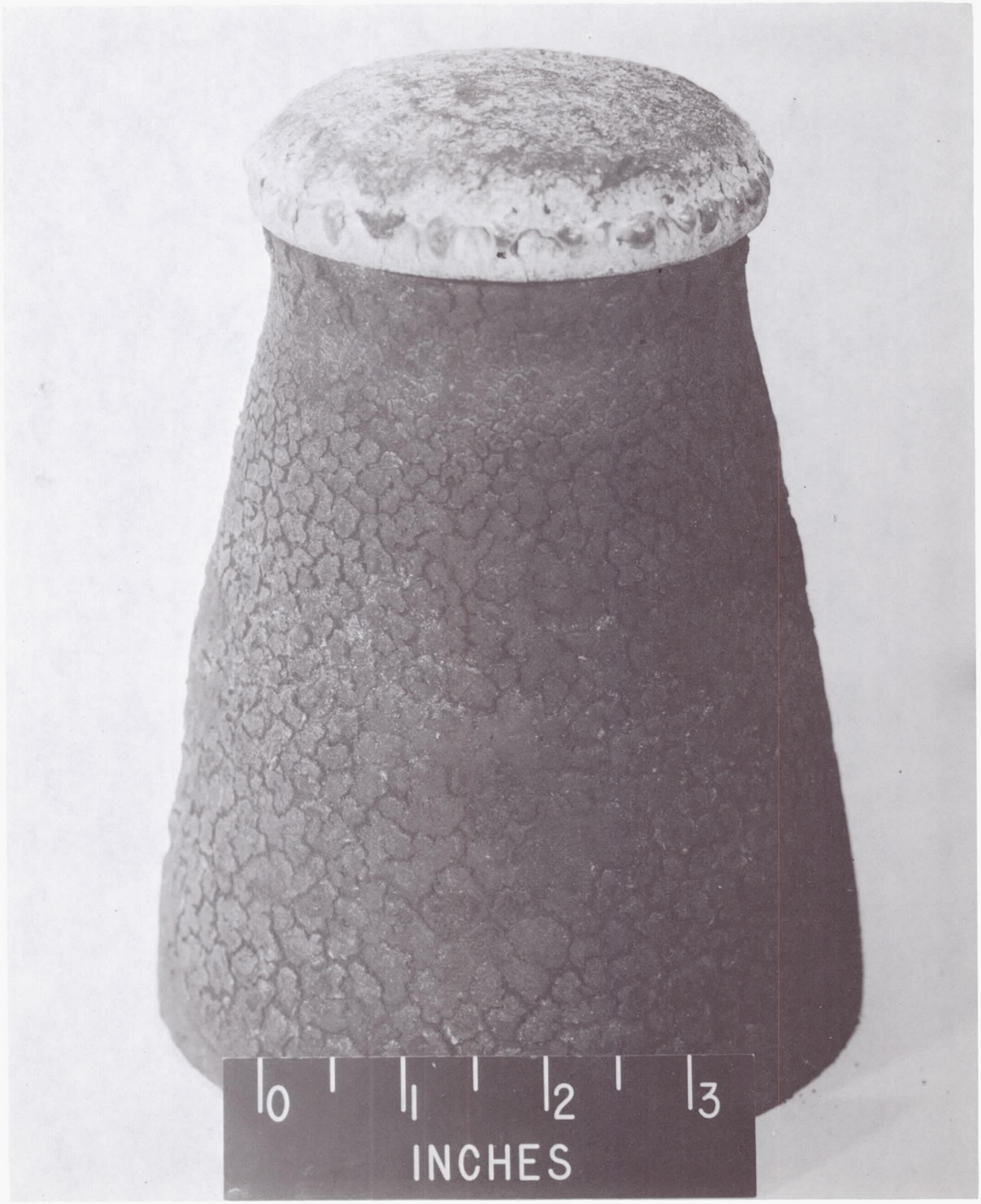

(b) Cork.

L-66-2560

Figure 10.- Continued.

(c) Avcoat 5026-39.

L-66-2559

Figure 10.- Continued.

(d) NASA E4A1.

L-66-2562

Figure 10.- Continued.

(e) Narmco 4032-C. L-66-2564

Figure 10.- Continued.

(f) Phenolic nylon. L-66-2563

Figure 10.- Continued.

(g) Narmco 4028.

L-66-2558

Figure 10.- Concluded.

NATIONAL AERONAUTICS AND SPACE ADMINISTRATION
WASHINGTON, D. C. 20546

OFFICIAL BUSINESS

FIRST CLASS MAIL

POSTAGE AND FEES PAID
NATIONAL AERONAUTICS AND
SPACE ADMINISTRATION

POSTMASTER: If Undeliverable (Section 158
Postal Manual) Do Not Return

"The aeronautical and space activities of the United States shall be conducted so as to contribute . . . to the expansion of human knowledge of phenomena in the atmosphere and space. The Administration shall provide for the widest practicable and appropriate dissemination of information concerning its activities and the results thereof."

—NATIONAL AERONAUTICS AND SPACE ACT OF 1958

NASA SCIENTIFIC AND TECHNICAL PUBLICATIONS

TECHNICAL REPORTS: Scientific and technical information considered important, complete, and a lasting contribution to existing knowledge.

TECHNICAL NOTES: Information less broad in scope but nevertheless of importance as a contribution to existing knowledge.

TECHNICAL MEMORANDUMS: Information receiving limited distribution because of preliminary data, security classification, or other reasons.

CONTRACTOR REPORTS: Scientific and technical information generated under a NASA contract or grant and considered an important contribution to existing knowledge.

TECHNICAL TRANSLATIONS: Information published in a foreign language considered to merit NASA distribution in English.

SPECIAL PUBLICATIONS: Information derived from or of value to NASA activities. Publications include conference proceedings, monographs, data compilations, handbooks, sourcebooks, and special bibliographies.

TECHNOLOGY UTILIZATION PUBLICATIONS: Information on technology used by NASA that may be of particular interest in commercial and other non-aerospace applications. Publications include Tech Briefs, Technology Utilization Reports and Notes, and Technology Surveys.

Details on the availability of these publications may be obtained from:

SCIENTIFIC AND TECHNICAL INFORMATION DIVISION

NATIONAL AERONAUTICS AND SPACE ADMINISTRATION

Washington, D.C. 20546